Heat Transfer of Swirling Multi Jets Impinging System

Amar Zerrout[*]*, Ali Khelil, Larbi Loukarfi*
Control Laboratory, Test, Measurement and Mechanical Simulation,
University of Chlef, Algeria, BP 151
**zerroutamar@yahoo.fr*

ABSTRACT

This work is the subject of an experimental and a numerical study of a system of swirling jets system impinging a plane wall. The experimental test bench comprising three diameter D diffusers, which are 2D distant between the axes, impacting perpendicular plate, by setting the impact height H = 4D. The swirl is obtained by a generator (swirl) of compound 12 fins arranged at 60 ° relative to the vertical placed just at the exit of the diffuser. A portable VELOCICALC PLUS anemometer device at various stations measures the blowing temperature of the swirling jets hitting the plate. The results of this study have shown that, the global jet has the same characteristics as a free jet, close to the obstacle it undergoes a considerable deviation characterized by the weakening of the temperature and the speeds then the development of the jet. The temperature amplitudes decrease, as we approach the plate. The velocity profiles show that velocity changes direction and increases radially. The Nusselt number is moderate at the level of the impact surface ensuring the homogenization of the heat transfer of the plate. The system was simulated numerically by the Fluent program based on the turbulence model (k-epsilon). The latter gave results of temperature and velocity fields having profiles in line with those of experimental results.

Keywords: *Turbulent swirling jet, impinging a plaque, thermal homogenization, ventilation, (k-epsilon) model.*

Nomenclatures

D: Diameter of the diffuser [m]
d: Diameter of the valve diffuser support [m]
D_{hy}: Hydraulic diameter [m]
H: Impact height [m]

ISSN 1823-5514, eISSN2550-164X

Received for review: 2019-11-21
Accepted for publication: 2020-03-26
Published: 2020-07-15

G_θ : Flux of angular momentum [$m^4.s^{-2}$]
G_x : Flux of Axial momentum [$m^4.s^{-2}$]
R: Radius of the diffuser [m]
r, X : Dimensional cylindrical coordinates [m]
Nu: Nusselt Number [-]
R_h : Radius of the valve diffuser support [m]
R_n : The radius of diffuser [m]
Re: Reynolds number [-]
S: Swirl number [-]
T_a : Ambient temperature [°C]
Ti : Jet temperature at the point considered. [°C]
T_r : Reduced temperature [-]
Tm : Maximum temperature at the outlet of the diffuser [°C]
U: Velocity in the axial direction [$m.s^{-1}$]
U_m: Maximum velocity at the exit of the diffuser [$m.s^{-1}$]
U_r : Reduced dimensionless axial velocity. [-]
U_i : Jet velocity at the point considered [$m.s^{-1}$]
V: Velocity in the radial direction [$m.s^{-1}$]
W: Velocity in the tangential direction [$m.s^{-1}$]
α: Inclination angle of the vanes [°deg].

Introduction

Several research papers have treated the convective transfer of free jet and confined flows, the swirling flow characteristics through an air jet impinging on flat surfaces or complex geometry, in order to improve the transfer of heat or localized mass in a portion of a system. This type of configuration is used in particular for anti-icing systems for aircraft turbojet engines as shown in Figure 1, for cooling electronic components, blading turbines, or quenching metallurgical and glass flows, as well as in convective drying of tunnels. A method commonly used in the aeronautical field for anti-ice operations of the front part turbojet engines of airplanes using hot air jet impinging the walls of frosted internal power of the engine as shown in Figure 1. For this, it is necessary to know the structure of the impinging jet in Figure 2, and the parameters that influence this behavior.

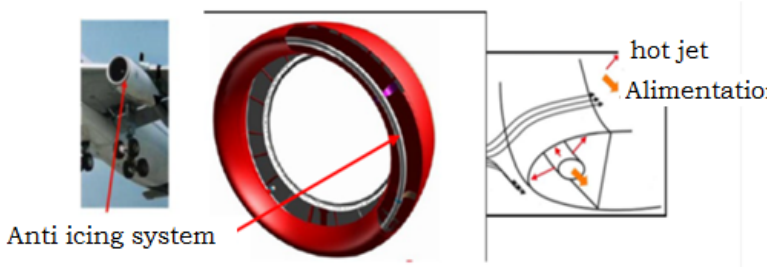

Figure 1: Anti-icing of the turbojet engine by impacting jets [1]

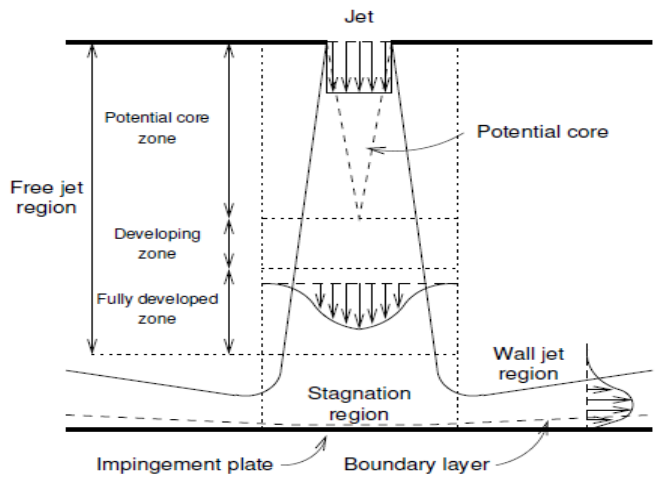

Figure 2: Flow configuration of a round impinging jet with regions of different flow regimes [2]

This section presents an overview of the current knowledge of the flow and heat transfer of both single impinging jets and multiple impinging jet arrays. First, the hydrodynamics of a single jet are described, followed by the flow features of multiple jet arrays. Next, single and multiple jet heat transfer is discussed. The dependencies of the Nusselt number on geometrical parameters and the temperature of the jet are discussed based on non-dimensional correlations.

Figure 2 shows the flow of an impinging jet issuing from a nozzle in a flat plate. An impinging jet is commonly divided into three regions based on the flow structure: the free jet region, the stagnation region, and the wall jet region.

Experimental setup

The realized experimental device as shown in Figure 3 composed of a frame of the cubic shape of metal; having at its upper part the hot air blowing apparatus (hairdryer), directed from the top downwards and in its lower part a diffuser (1) according to configuration studied. This device allows scanning the maximum space provided by a particular arrangement of the rods supporting the temperature sensors (2); the temperature field is explored through a portable anemometer device VELOCICALC PLUS (3). Easily guided rods support the sensors vertically and horizontally to sweep the maximum space, a horizontal plate (4) Formica material, the temperature and velocity fields are measured in different stations in the axial directions and radial flow.

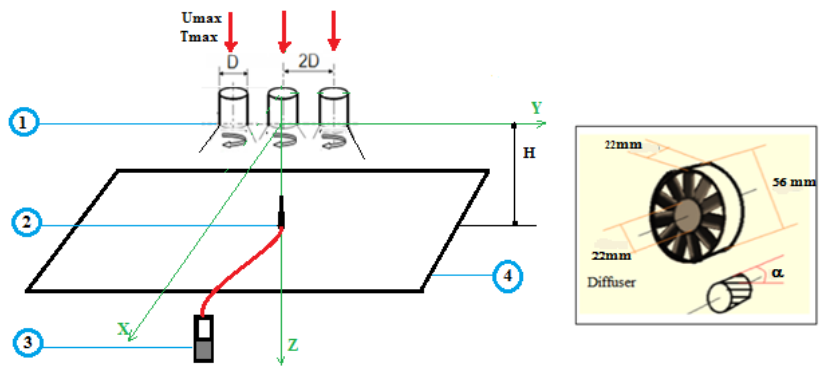

Figure 3: Experimental configuration and visualization of digital sensors [3]

The Number of Swirl

A dimensionless number that defines a measure of the ratio between the angular momentum of the axial flow and axial momentum characterizes the swirl [4].

$$S = \frac{G_\theta}{RG_X} = \frac{\int_0^R r^2 UW dr}{R\int_0^R r\left(U^2 - \frac{W^2}{2}\right)dr} \quad (1)$$

The swirl number can be evaluated at any position of the jet because the two quantities are calculated. Swirling helps promote and improve the process

of mixing and transfer, as well as the jet has the advantage of quickly flourish in free jets.

Another empirical formula is used for calculating the number of swirl that the swirl number defined according to the geometric parameters of the swirl generator. This number S can be written as follows [5]:

$$S = \frac{2}{3}\left[\frac{1-\left(\frac{R_h}{R_n}\right)^3}{1-\left(\frac{R_h}{R_n}\right)^2}\right].tg\alpha \tag{2}$$

Such that:

α: is the angle of the fins built swirl generator (see Figure 3),

R_h : is the radius of the vane diffuser support,

R_n : is the radius of diffuser.

Note that in the case of a swirler hub withouta nucleus ($R_h = 0$), the expression becomes [6]:

$$S = \frac{2}{3}tg\alpha \tag{3}$$

In this study, the axial and tangential velocities *U* and *W*, respectively, were measured at the outlet of a diffuser with a swirling jet hot wire anemometer triple probes (DISA55M01). Four values of the swirl number can be used, S = 0 to α = 0°, S = 0.4 to α = 30°, S = 0.7 to α = 45° and S =1.3 to α = 60°, respectively. According to reference [7], the swirl number is used, which corresponds to α = 60°.

Operating Conditions

The experimental setup was placed in a laboratory room isolated from the outside air, having the following dimensions: length = 4 m, width =3.5 m and height = 3 m. There must be a free flow of the isolation and testing, the initial temperature at the blowing port was 90 °c for each jet.

Measurement Procedure

The values of the initial flowing temperature (Ti) and the value of the ambient temperature (Ta) is measured by precision temperature sensors (1/100). It is noted that when the temperature stabilizes, with a delay ten minutes was sufficient to achieve this stabilization, after measuring, the temperatures for a

given configuration, the blowing sail is stopped and preceded to the movement of the rods door probes to other measurement point.

Dimensionless Quantities

The reduced temperature of measurement is obtained by reference to the maximum average temperature at the outlet of the blowing port and the room temperature:

$$T_r = \frac{T_i - T_a}{T_{max} - T_a} \tag{4}$$

The reduced dimensionless axial velocity is obtained from the maximum speed to the outlet of the blowing port.

$$U_r = \frac{U_i}{U_{max}} \tag{5}$$

The radial and axial distances are given by reference to the diameter of the blow port as dimensionless r/D and x/D.

Numerical Procedure

The Turbulence Model (k-ε) Standard

The turbulence model (K-ε) is a model of turbulent viscosity in which Reynolds stresses are assumed to be proportional to the gradient of the average velocity, with a proportionality constant representing the turbulent viscosity. This hypothesis, known by the name the assumption of "Boussinesq" provides the following expression for the stress tensor Reynolds [8]:

$$\overline{\rho u_i' u_j'} = \rho \frac{2}{3} k \delta_{ij} - \mu_t \left(\frac{\partial u_i}{\partial x_j} + \frac{\partial u_j}{\partial x_i} \right) + \frac{2}{3} \mu_t \frac{\partial u_i}{\partial x_i} \delta_{ij} \tag{6}$$

Here it is the turbulent kinetic energy defined by:

$$k = \frac{1}{2} \sum_i \overline{u_i'^2} \tag{7}$$

Eddy viscosity is obtained by assuming that it is proportional to the product of the scale of the turbulent velocity and length scale. In (k-ε) model,

these scales velocities and lengths are obtained from two parameters k and the kinetic energy dissipation rate. So can express by the following relation:

$$\mu_t = \rho C_\mu \frac{k^2}{\varepsilon} \tag{8}$$

With: $C_\mu = 0{,}09$ (empirical constant).

k values and $\boldsymbol{\varepsilon}$ required in the equation are obtained by solving the following conservation equation:

$$\begin{aligned}
&\frac{\partial}{\partial t}(\rho k)+\frac{\partial}{\partial x_j}(\rho u_i k)=\frac{\partial}{\partial x_j}\left(\left(\mu+\frac{\mu_t}{\sigma_k}\right)\frac{\partial k}{\partial x_j}\right)+G_k+G_b-\rho\varepsilon+S_k \\
&\frac{\partial}{\partial t}(\rho \varepsilon)+\frac{\partial}{\partial x_j}(\rho u_i \varepsilon)=\frac{\partial}{\partial x_j}\left(\left(\mu+\frac{\mu_t}{\sigma_k}\right)\frac{\partial \varepsilon}{\partial x_j}\right)+G_{1\varepsilon}\frac{\varepsilon}{k}(G_k-C_{3\varepsilon}.G_b)-C_{2\varepsilon}\rho\frac{\varepsilon^2}{k}+S
\end{aligned} \tag{9}$$

Such as:

$C_{1\varepsilon} = 1.44$ and $C_{2\varepsilon} = 1.92$: empirical constants.

$\sigma_k = 1.0$ and $\sigma_\varepsilon = 1.3$: numbers of Prandtl for k and ε respectively.

S_k and S_ε : are terms for sources k and ε respectively.

G_k: represent the generation of the turbulent kinetic energy due to the average velocities gradient.

$$G_k = \mu_t\left(\frac{\partial u_j}{\partial x_i}+\frac{\partial u_i}{\partial x_j}\right)\frac{\partial u_j}{\partial x_i} \tag{10}$$

G_b: Coefficient generation of turbulence due to the entrainment.

$$G_b = -g_i \frac{\mu_t}{\rho\sigma_h}\frac{\partial \rho}{\partial x_i} \tag{11}$$

Domain Calculating and Mesh

The computational domain is divided into a number of volumes called no superposed control volume such that each volume surrounding each point of the mesh. The differential equation is integrated for each volume control and the result of this integration gives the discrete equation expressed using the values of the function ϕ (scalar quantity) for a set of grid points. The discrete

equation obtained expresses the principle of conservation for ϕ on the volume control in the same manner that the differential equation expressed for an infinitesimal volume control [9].

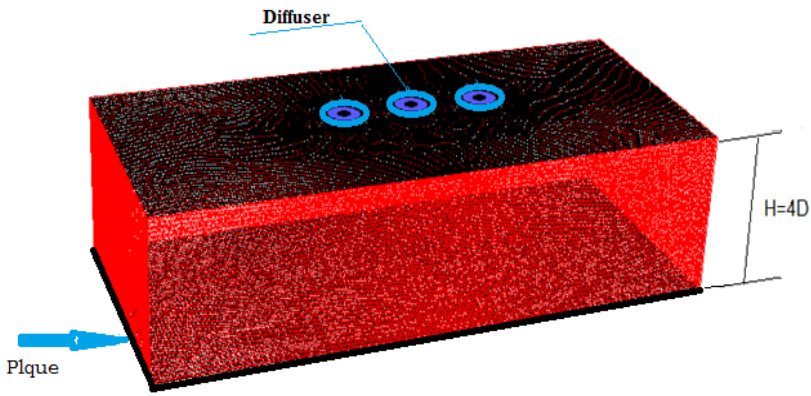

Figure 4: Domain calculating and mesh geometry for three diffusers with hauteur of impact 4D

Calculations were tested on various meshes for the control of the solution, in order to seek the limit of the independence of the solution compared to the fineness of the mesh, with meshes of tetrahedral form, a number of 865421 cells and a number 166655 nods. We can therefore conclude that the mesh is acceptable and the solution is independent of the mesh. An entry condition for the pressure outlet type diffuser, with an entry speed of U = 10 ms^{-1}, and a temperature T0 = 363 °K, a hydraulic diameter D_{hyd} = 0.047 m, the Reynolds number Re = 30,000. At the exit, a pressure outlet type condition is set. The plate having dimensions of 450 x 100 mm.

Numerical Results

Reduced Temperature Profiles and Reduced Velocity Profiles

We will present the results, reduced temperature profiles Tr and mean velocity profiles dimensionless Ur, depending on the ratio r/D in Figure 5 and Figure 6 for a single jet in relation to a height of impact H = 4D.

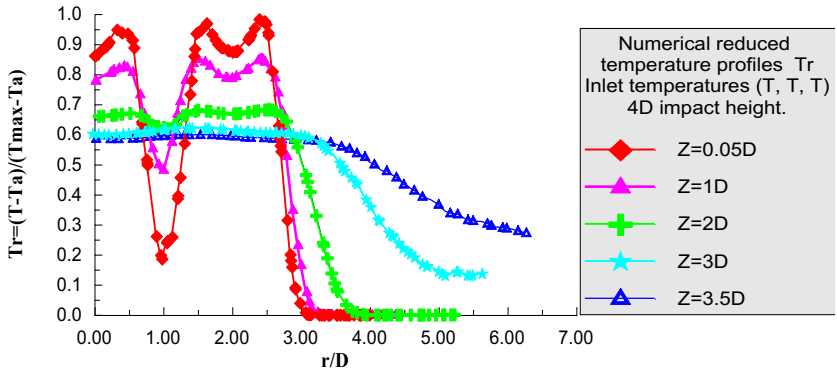

Figure 5: Profiles of the reduced temperature for a swirling turbulent jet with height impact 4D

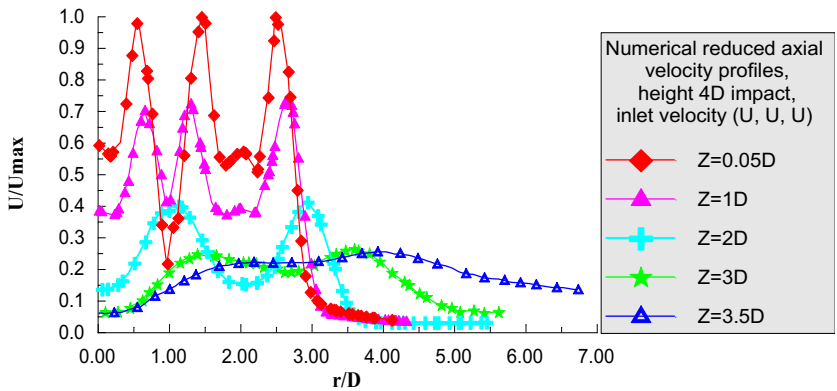

Figure 6: Profiles of the reduced velocity for a swirling turbulent jet with height impact 4D

We note that the curves of temperatures and velocities diminuend maximum amplitude potential heart level jet (close to the blowing port), to low amplitudes near the impact region. The reduced temperature tends towards the ambient temperature Ta, downstream of the jet. The mean velocity dimensionless Ur diminishes as one moves downstream and becomes almost parallel to the plate. Thus, the single jet has a low sprawl.

The increase in temperature and speed for r / D> 3 represents the deflection of the fluid on the impact surface in the radial direction.

Profiles of the Nusselt Number, Nu

The Nusselt number characterizes the heat transfer from the impinging jets. It is a dimensionless number that quantifies the heat transfer between a fluid and a wall of the baffle plate. It represents the ratio of convective exchanges on conductive exchanges [10].

$$Nu = \frac{h.D_{hy}}{\lambda} \tag{12}$$

Such as:
h: Local convective heat transfer coefficient [W.m-2.K-1]
λ: The thermal conductivity of air, taken at the reference temperature [W.m^{-1}.k^{-1}]
D_{hy}: hydraulic diameter [m]

As a general rule, the heat transfer correlations in this regime are described by the following equation:

$$Nu = C.Re^{m}.Pr^{n} \tag{13}$$

The constants C, m and n depend on the geometry of the jet and the geometry of the impact surface. The dimensionless numbers of Nusselt (Nu), Reynolds (Re) and Prandtl (Pr) take into account the thermo-physical properties of the fluid at its temperature at the nozzle outlet. Thermo physical properties are estimated at the temperature of the impinging jet.

Table 1: Correlations in the flow area

Authors	Flow regime	C	m	n	Reynolds values
McMurral et al.	Laminar	0.75	0.5	0.33	3.10^5
(1966)	Turbulent	0.037	0.8	0.33	3.10^5
Vader (1988)	Laminar	0.89	0.48	0.4	100--3.10^5
Robidou (2000)	Laminar	0.81	0.53	0.4	5000--6000
Kouachi	Turbulent	0.042	0.78	0.33	104--10^5

According to, Me Murray et al. [11] for a turbulent flow C = 0.037, m = 0.8 and n = 0.33. From where:

$$Nu = 0.037\ \ Re^{0.8}(Pr)^{0.33} \tag{14}$$

Re is the Reynolds number. It is defined by:

$$Re = \frac{\rho.U.D_{hy}}{\mu} \tag{15}$$

Where;

ρ : density of air [kg.m-3]

U: average velocity [m.s-1]

D_{hy}: hydraulic diameter [m]

Pr: Prandtl number is a dimensionless number; it represents the ratio of momentum diffusivity and thermal diffusivity.

$$Pr = \frac{\mu.Cp}{\lambda} \tag{16}$$

μ: dynamic viscosity [N.s.m-2]

Cp : specific heat [J.kg-1.K-1]

λ : air thermal conductivity en [W.m-1.k-1]

Figure 7 shows the superposition of the Nusselt Nu number profiles, whose impact height is H = 4D, for an inlet velocity in the diffusers (U, U, U) and an inlet temperature (T, T, T). Initially, the Nusselt profiles indicate peaks at the blast port and disturbances. These disturbances are due to the support of the fins. Amplitudes and disturbances decrease progressively as we move downstream of the jet. At station Z = 3.5D, the number of Nusselt is moderate at the level of impact surface ensuring homogenization of heat transfer plate.

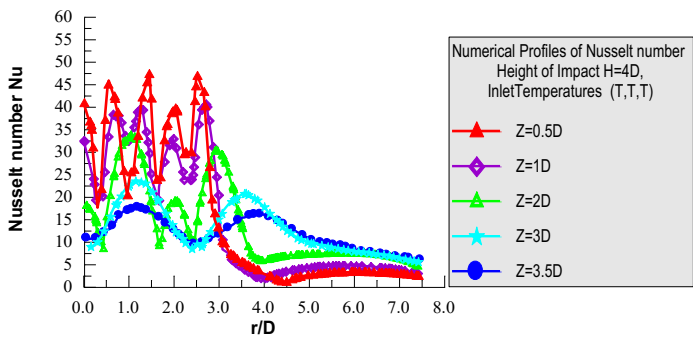

Figure 7: Profiles of the Nusselt number Nu depending of the dimensionless distance r/D

Temperature field and velocity vectors

Figure 8 illustrates the temperature and velocity vector field in the (y, z) plane of a three-jet system, for an impact height H = 4D, relative to an input temperature distribution (T, T, T). Note that it has symmetry with respect to the z-axis. The potential cone is uniform for all three jets; the distribution of the temperature field is well balanced over the entire domain. For the velocity field in the impact region, a deflection zone appears, so that the velocities change from the axial direction to the radial direction.

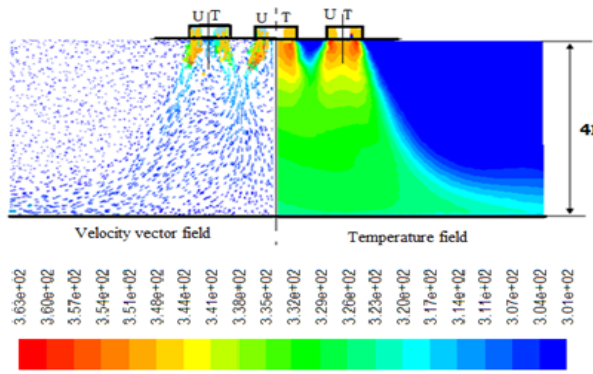

Figure 8: Temperature field and velocity vectors

Figure 9 shows the temperature field lines being symmetrical with respect to the main axis of the jet, an entire and balanced propagation of the heat transfer over the entire domain, the temperature reaches the entire surface of the plate, which favours homogeneity thermal transfer over the entire surface of the plate.

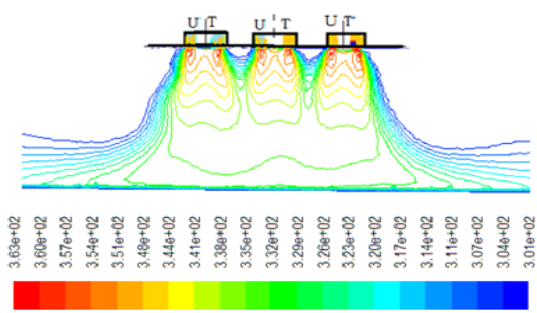

Figure 9: Temperature field lines

Figure 10 shows the contours temperature fields on the wall of the heated plate by a system of three jets impacting the plate at a height H = 4D, with the inlet temperatures of the diffuser (T, T, T). It should be noted that in the figure this distribution of the temperature field is distributed symmetrically and almost over the entire surface of the plate. Thus, it promotes the homogeneity of the heat transfer over the entire surface of the plate.

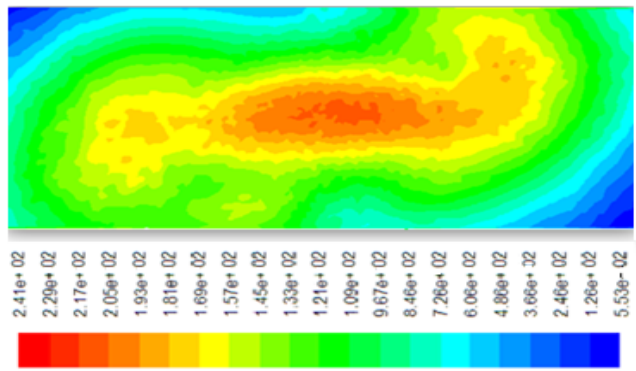

Figure 10: Contour temperature field of the plaque

Validation of Results

The quality of comparison between the numerical results and experimental results comparison is evidenced in Figures 11 on the inlet temperature Tr, at the reduced velocity Ur in the (y, z), respectively. The numerical results of the model with two transport equations (K-ε) used to simulate this case, are in good agreement with experimental results. However a smaller gap in the first station. The model (K-ε) considers an isotropic turbulent viscosity.

Without omitting the influence of uncertainties of measurements operated on. Despite the shortcomings, the model (K-ε) gave acceptable results qualitatively. Nevertheless, it is a relatively simple and inexpensive simulation tool.

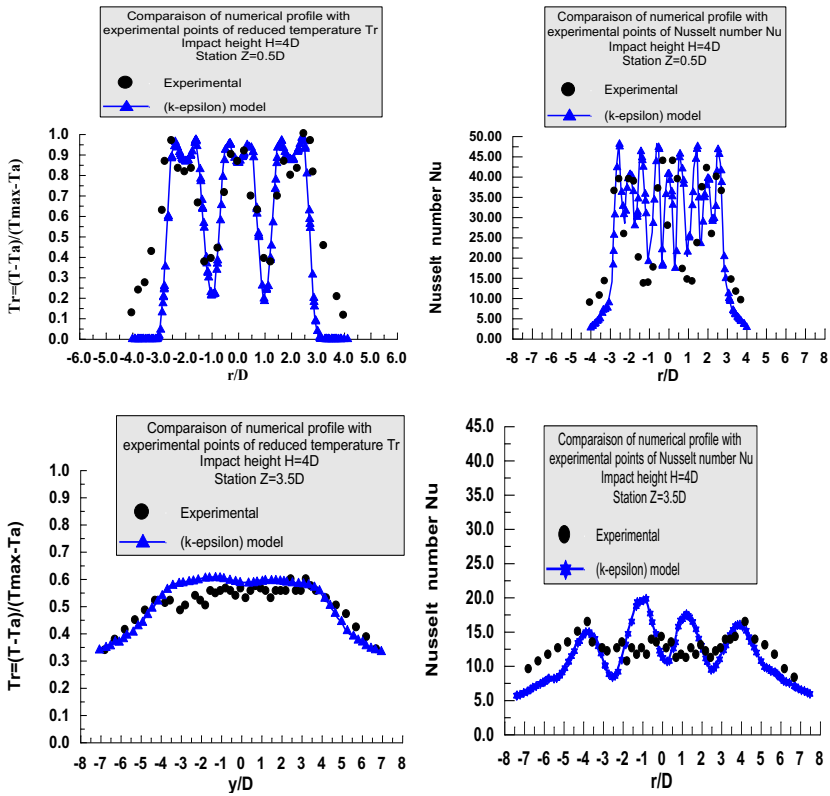

Figure 11: Comparison of numerical and experimental profiles of the reduced temperature Tr and Nusselt number for stations (0.5D and 3.5D) in the (r, z), with height of impact 4D

Conclusion

The results of this study show that initially, the resulting jet has the same characteristics as a free jet. Near the obstacle that it undergoes a considerable deviation characterized by the weakening of the speed and the development of the jet (With the temperature and velocity amplitudes decreasing as one approaches the plate). In contact with the plate, the temperature and velocity curves are almost parallel to the plate. The velocities change direction and would grow radially. The swirling ensures a uniform distribution of the heat with a complete diffusion of the jet. It slows the fluid particles and promotes better jet development to provide better heat transfer and uniform temperature

distribution along the plate. The presence of the plate decreases the differences in the temperature of the jet, the temperature of the plate decreases gradually downstream of the jet as one approaches the plate. The number of Nusselt is moderate at the impact surface level ensuring homogenization of heat transfer plate. The comparison between the numerical results and the experimental results presented in this study indicates that the model with two equations of transport (K-) has produced satisfactory results. Despite the weaknesses of this model, the latter has given acceptable results on the comparison plan. It remains a relatively simple and inexpensive simulation tool to use.

References

[1] P. Reulet, R Phibel, P. Grenard, "Comparison calculations experiments on the cooling impact of subsonic jets," SFT day, March 9. 16. Paris, 2006.

[2] R. Viskanta, "Turbulent flow in the near field of a round impinging jet", International Journal of Heat and Mass Transfer 54(23), 4939-4948 (2011).

[3] A. Zerrout, A. Khelil, L. Loukarfi, "Numerical study of a three swirling jets system impacting a plane plate", Control Laboratory, Test, Measurement and Mechanical Simulation, University of Chlef, Algeria, Journal of Mechanics & Industry (2016).

[4] A. K. Gupta, D.G. Lilley, N. Syred, "Swirl flows", London: Abacus Press (1984).

[5] Y. Huang, V. Yang, "Dynamics and Stability of Lean-Premixed Swirl-Stabilized Combustion", Progress in Energy and Combustion Science, 35 (4), 293-364 (2009).

[6] H. Saato, M. Mori, T. Nakamura, "Development of a Dry Ultra-low NOx Double Swirler Staged Gas Turbine Combustor," Journal of Engineering for Gas Turbine and Power. January 120, (1998).

[7] M. Braikia, L. Loukarfi, A. Khelil, and H. Naji, "Improvement of thermal homogenization using multiple swirling jets," Université Lille Nord de France, Thermal Science 16 (1), 239-250.

[8] B.E. Launder, D.B. Spalding, "Mathematical models of turbulence", Dept of Mechanical Engineering, Imperial Collogue of Science and Technology, London. England (1972).

[9] Dimh. Vo. Ngoc, Dinh. Vo. Ngoc, "Numerical methods of local integral on finite volumes", School of Engineering, University of MONCTON. CANADA (1989).

[10] G. Wigley, J.A. Clark, "Heat transport coefficients for constant energy flux models of broad leaves", Boundary Layer Meteorology 139-150 (1974).

[11] D.C. Mc Murray, P.S. Myers, O.A. Uyehara, “Heat Transfer Conference”, in proceeding 2, 292 (1966).
[12] FLUENT User’s Guide, 2006.